N73-16774
NASA TM X-2708

NASA TECHNICAL MEMORANDUM

NASA TM X-2708



# EXPERIMENTAL INVESTIGATION OF A 2.5-CENTIMETER-DIAMETER KAUFMAN MICROTHRUSTER

*by Allan J. Cohen*
*Lewis Research Center*
*Cleveland, Ohio 44135*

NATIONAL AERONAUTICS AND SPACE ADMINISTRATION • WASHINGTON, D. C. • FEBRUARY 1973

| 1. Report No. NASA TM X-2708 | 2. Government Accession No. | 3. Recipient's Catalog No. |
|---|---|---|
| 4. Title and Subtitle EXPERIMENTAL INVESTIGATION OF A 2.5-CENTIMETER-DIAMETER KAUFMAN MICROTHRUSTER | | 5. Report Date February 1973 |
| | | 6. Performing Organization Code |
| 7. Author(s) Allan J. Cohen | | 8. Performing Organization Report No. E-7127 |
| | | 10. Work Unit No. 502-24 |
| 9. Performing Organization Name and Address Lewis Research Center National Aeronautics and Space Administration Cleveland, Ohio 44135 | | 11. Contract or Grant No. |
| | | 13. Type of Report and Period Covered Technical Memorandum |
| 12. Sponsoring Agency Name and Address National Aeronautics and Space Administration Washington, D.C. 20546 | | 14. Sponsoring Agency Code |
| 15. Supplementary Notes | | |

16. Abstract

A 2.5-centimeter-diameter Kaufman electron bombardment microthruster was fabricated and tested. The microthruster design was based on the 15-centimeter-diameter SERT II and 5-centimeter-diameter Lewis experimental thruster designs. The microthruster with a two-grid system, operating at a net accelerating potential of 600 volts and an accelerator potential of 500 volts, produced a calculated 445-$\mu$N (100-$\mu$lbf) thrust when it was run with a 9-milliampere beam current. A glass grid was initially used in testing. Later a two-grid system was successfully incorporated. Both the propellant utilization efficiency and the total power efficiency were lower than for large-size advanced thrusters, as expected; but they were sufficiently high that 2.5-centimeter thrusters show promise for future space applications. Total power of the microthruster with an assumed 7-watt hollow-cathode neutralizer was less than 30 watts at a thrust level of 445 $\mu$N (100 $\mu$lbf). The hollow cathode was operated at zero tip heater power for power requirement tests.

| 17. Key Words (Suggested by Author(s)) | 18. Distribution Statement |
|---|---|
| Microthruster<br>Mercury ion thruster<br>Ion thruster<br>Bombardment thruster | Unclassified - unlimited |

| 19. Security Classif. (of this report) | 20. Security Classif. (of this page) | 21. No. of Pages | 22. Price* |
|---|---|---|---|
| Unclassified | Unclassified | 22 | $3.00 |

* For sale by the National Technical Information Service, Springfield, Virginia 22151

# EXPERIMENTAL INVESTIGATION OF A 2.5-CENTIMETER-DIAMETER KAUFMAN MICROTHRUSTER

by Allan J. Cohen

Lewis Research Center

## SUMMARY

A 2.5-centimeter-diameter Kaufman electron bombardment microthruster was fabricated and tested. The microthruster design was based on the 15-centimeter-diameter SERT II and 5-centimeter-diameter Lewis experimental thruster designs. The microthruster with a two-grid system, operating at a net accelerating potential of 600 volts and an accelerator potential of 500 volts, produced a calculated 445-micronewton (100-$\mu$lbf) thrust when it was run with a 9-milliampere beam current. A glass grid was initially used in testing. Later a two-grid system was successfully incorporated. Both the propellant utilization efficiency and the total power efficiency were lower than for large-size advanced thrusters, as expected; but they were sufficiently high that 2.5-centimeter thrusters show promise for future space applications. Total power of the microthruster with an assumed 7-watt hollow-cathode neutralizer was less than 30 watts at a thrust level of 445 micronewtons (100 $\mu$lbf). The hollow cathode was operated at zero tip heater power for power requirement tests.

## INTRODUCTION

Electric thrusters of various designs have been researched and developed for a period of about a decade. Some electric thrusters with thrust levels in the micronewton (micropound) range have become operational as auxiliary propulsion devices on spacecraft (ref. 1). Prior to this work, the smallest mercury electron bombardment thruster was a 5-centimeter-diameter (5-cm) thruster with a 1780-micronewton (400-$\mu$lbf) thrust level. This thruster has been developed by the Lewis Research Center and the Hughes Research Center (refs. 2 and 3) for space application. At this thrust level a 5-cm electrostatic thruster could be used for the auxiliary propulsion role of north-south stationkeeping for a 350-kilogram (770 lbm) synchronous spacecraft (ref. 4). Smaller electric thrusters with lower thrust levels may be required for east-west stationkeeping and attitude control of a synchronous spacecraft (ref. 4).

In this report, descriptions of tests made with a 2.5-centimeter-diameter (2.5-cm) Kaufman thruster using mercury propellant and operated at a nominal thrust level of 445 micronewtons (100 $\mu$lbf) are presented. This thruster is the smallest mercury electron bombardment thruster tested to date at the Lewis Research Center. The thruster design is based on designs of the SERT II thruster (ref. 5) and those of the 5-cm thruster previously mentioned.

To be competitive with existing systems, an electric microthruster must have low operating power, high reliability, and long life. The latter two requirements should be partially satisfied if the 2.5-cm microthruster can be operated in a manner similar to that of the flight-tested SERT II thruster (refs. 6 and 7). To achieve a low operating power level, however, a low-specific-impulse grid system and low-powered hollow cathodes must be used. For a power level goal of less than 30 watts for 445-micronewton (100-$\mu$lbf) thrust operation, the two hollow cathodes of the microthruster should be operated at less than about 5 watts each. This is lower than the operating value in the SERT II program.

In this microthruster program, tests were conducted on two 2.5-cm thrusters using two different low-specific-impulse grid systems. First, a microthruster with a glass grid was performance tested, and power requirements were noted. Second, a somewhat longer microthruster incorporating a low-specific-impulse, two-grid system was operated. Performance and power requirements were recorded and are presented in this report.

## APPARATUS AND PROCEDURE

### Thruster Design

Figures 1 and 2 are schematics of the two thruster designs tested in the program. Both thruster designs had an anode diameter of 2.5 centimeters. The short thruster (fig. 1) had a discharge-chamber-length-to-anode-diameter ratio of 0.6, while the long thruster (fig. 2) had a ratio of 1.0. The dimensions of the mild-steel collar and the pole piece were the same for both thruster designs. The collar extended 0.6 centimeter back on the chamber body. The cathode pole piece had an inner diameter of 0.8 centimeter and a length of 0.4 centimeter. Like the 5-cm thruster (refs. 2 and 3), this thruster had a cathode pole piece with an open-side configuration, as shown in figure 1. This pole piece was fabricated from six mild-steel rods set in the backplate, forming a circle and capped with a mild-steel ring. The open sides of the cathode pole piece were

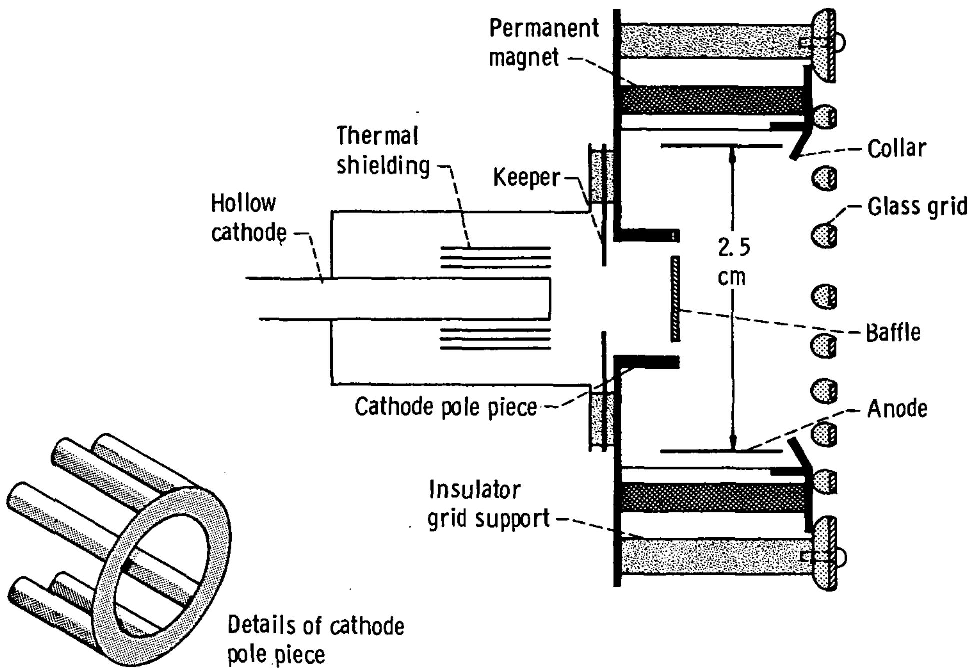


Figure 1. - Short thruster with a glass-coated grid.

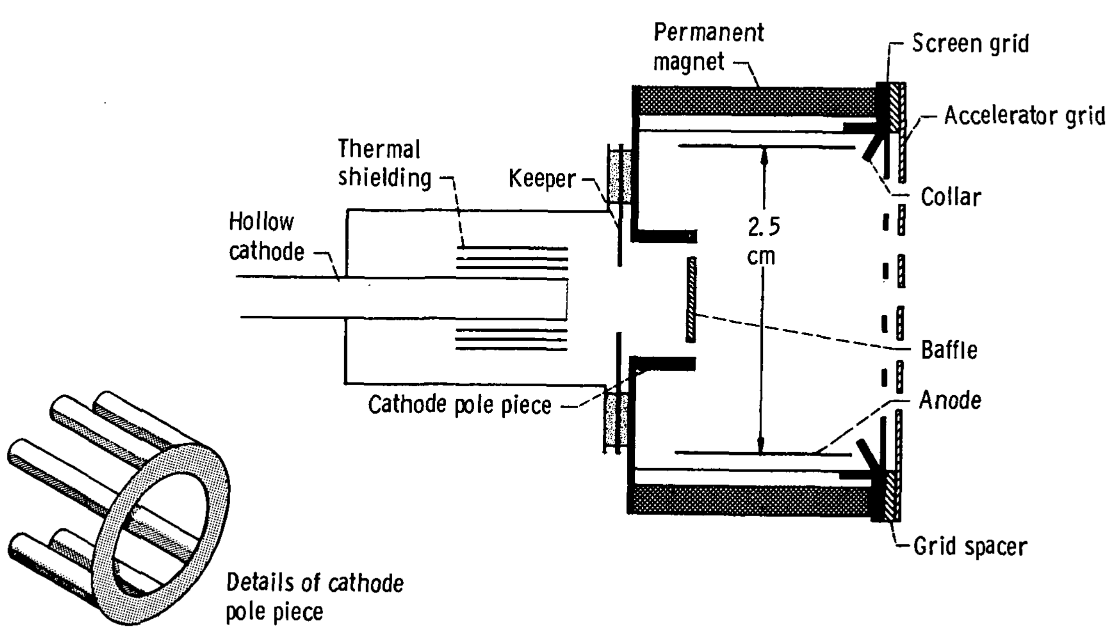


Figure 2. - Long thruster with two metal grids.

wrapped with a stainless-steel mesh. Both thruster designs used a solid disk-shaped baffle 0.47 centimeter in diameter. It was supported by three wires in the position shown in figures 1 and 2. The mercury flow for both thrusters entered the chamber through the hollow cathode. The combination of the baffle and the open-side cathode pole piece was designed to distribute the mercury vapor, a technique that has shown good chamber performance (ref. 2).

The short thruster used seven 0.312-centimeter-diameter permanent magnets which gave a measured magnetic-field strength of 10.4 millitesla (104 G) in front of the baffle on the thruster centerline. The long thruster used 12 similar-diameter permanent magnets. The measured magnetic-field strength was 22.0 millitesla (220 G) at the same point. The use of a stronger magnetic field in the long thruster was based on the author's experience with discharge-chamber, magnetic-field interaction.

The keeper was made from a 0.25-millimeter-thick tantalum sheet in the form of a disk with a hole in it. It was sandwiched between two insulating sheets and placed as shown in figures 1 or 2. The keeper, in conjunction with the hollow-cathode holder, essentially formed an enclosed keeper design like that used in the 5-cm thruster. Keeper holes of 0.625 centimeter or 0.312 centimeter were used.

## Thruster Grid Systems

Two thruster grid systems were used in the project. The first system was a glass-coated grid, which was operated on the short thruster. The base for the glass was a molybdenum, perforated, circular sheet that had a thickness of 0.025 centimeter. The perforations were a hexagonal array of circular holes 0.125 centimeter in diameter. The distance from hole center to hole center was 0.165 centimeter, with a minimum webb thickness of 0.040 centimeter. The open area of the perforated molybdenum sheet was 51 percent. As described in reference 8, a thermally compatible glass coating of nominally 0.050-centimeter thickness was bound to the upstream surface of the metal grid. Because the glass penetrated the holes, the open area with the glass coating was 33 percent. The holes in the glass grid extended somewhat beyond the 2.5-centimeter-diameter chamber. The remaining solid molybdenum sheet was also covered with a smooth glass coating to provide electrical insulation. The grid was mounted to three insulators, as shown schematically in figure 1, and was separated from the front of the collar by a 0.037-centimeter gap. Further information on this type of grid is found in reference 9.

The second grid system, used on the long thruster, consisted of two perforated molybdenum circular sheets: a screen grid butted to the collar, and a downstream accelerator grid (see fig. 2). The two grids were separated by a 0.050-centimeter-thick mica spacer. A hexagonal array of 0.187-centimeter-diameter holes was drilled into the screen grid with a hole-center-to-hole-center distance of 0.222 centimeter. A matching array of holes, 0.150 centimeter in diameter, was drilled into the accelerator. All holes in the screen grid and in the accelerator grid were contained inside a circle with a 2.5-centimeter diameter. The screen was 0.025 centimeter thick and the accelerator, 0.050 centimeter thick. The screen grid had a 65-percent open area compatible with present high-open-area, good-performance screen grids (ref. 5), while the accelerator open area was 42 percent.

## Hollow-Cathode Designs

The hollow cathode used in the two test series was a SERT II type that is described in reference 10. Briefly, it consisted of a 0.31-centimeter-diameter tantalum tube with a 2-percent-thoriated tungsten tip. An approximately 0.025-centimeter-diameter hole 1 millimeter long was sandblasted in the center of the tip.

A tungsten-rhenium heater coil placed close to the tip was embedded in a flame-sprayed aluminum oxide coating. A tantalum foil insert coated with barium carbonate was set into the cathode tube. For operation, the hollow cathode was wrapped with many layers of tantalum foil for the purpose of conserving heater power.

In the latter part of the second test series a slightly different hollow-cathode design was used. A commercially available, 80-percent-dense, porous tungsten tip was press fit into a molybdenum tube. Because the porous tungsten was impregnated with barium oxide, no barium-carbonate-coated insert was used. A 0.025-centimeter hole was sandblasted into the tip. Since it was found impossible to spot weld one side of the tungsten-rhenium heater coil to the molybdenum tube as in the SERT II heater design, a slip-on swaged heater was used. This heater - hollow-cathode configuration was inefficient even though a tantalum foil shield was used. Both hollow cathodes were affixed with a thermocouple at the side of the tip about 0.3 centimeter from the front edge with leads set below the tantalum foil.

## Electrical Setup

The microthruster was run off a power package schematically depicted in figure 3. The keeper, discharge, and accelerating power supplies were direct-current supplies with polarities as shown. The remaining were alternating-current heater supplies. The discharge power supply, as well as the keeper power supply, were current controlled. The keeper supply had a maximum output of 500 volts, while the discharge sup-

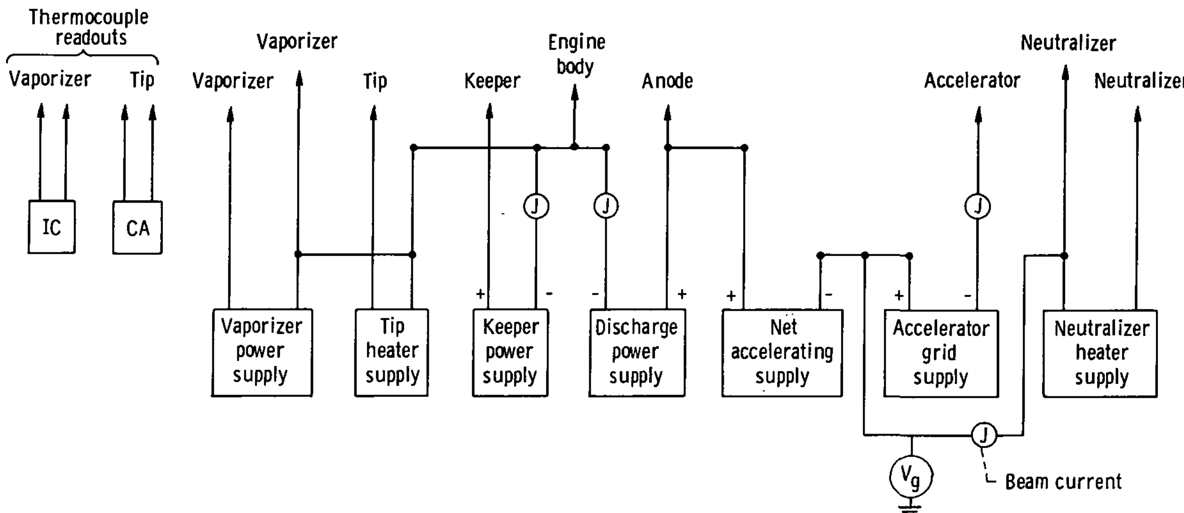


Figure 3. - Electrical block diagram of power package.

ply had a maximum output of 100 volts. The net accelerating voltage supply had a maximum output of 600 volts, but later was replaced by a 900-volt supply. The accelerator supply had a maximum output of 500 volts. For simplicity, a heated-tungsten-wire neutralizer was used throughout the program. The power supplies and thruster floated below ground to a voltage displayed by a voltmeter labeled $V_g$ in figure 3. A dummy load was used with two calibrated 1-percent-accurate meters to calibrate the power-package panel meters. Electrical-panel-meter data were accurate to ±3 percent.

## Facilities

The microthruster was run into a metal-and-screen enclosure placed in a bell jar, as shown in figures 4 and 5. The thruster was operated face down aimed at a stainless-steel conical beam target. The plasma beam was contained by the metal-and-screen enclosure to prevent it from affecting electrical readouts. The liquid mercury flow was measured by timing the fall in a true-bore glass tube. Estimated flow accuracy is ±10 percent. The flow rate was controlled by a heated porous vaporizer. The bell jar had a liquid-nitrogen-cooled plate and maintained pressures of $1\times10^{-5}$ to $2\times10^{-5}$ torr while the thruster was operating. In a later test the microthruster was operated in a short 30-centimeter-diameter port connected to a 1.1-meter-diameter tank. The tank pressure was $8\times10^{-6}$ torr with the thruster operating.

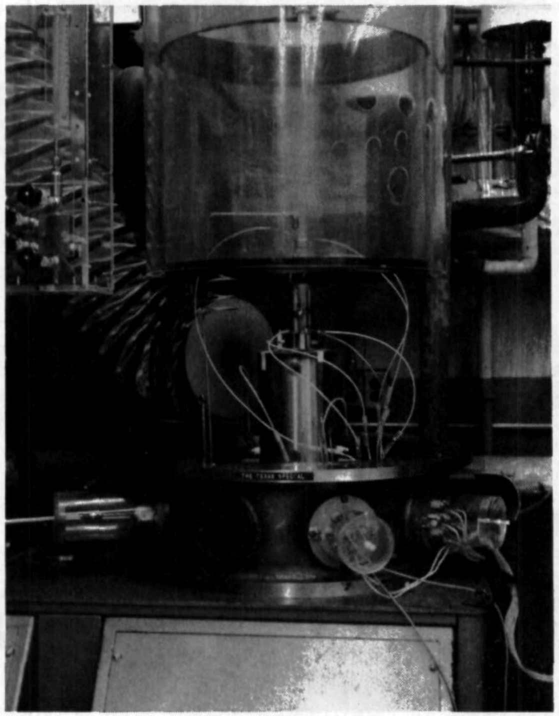

Figure 4. - Microthruster set on top of miniature tank placed in a bell jar, showing electrical leads, mercury feed lines, and cold trap (circular plate).

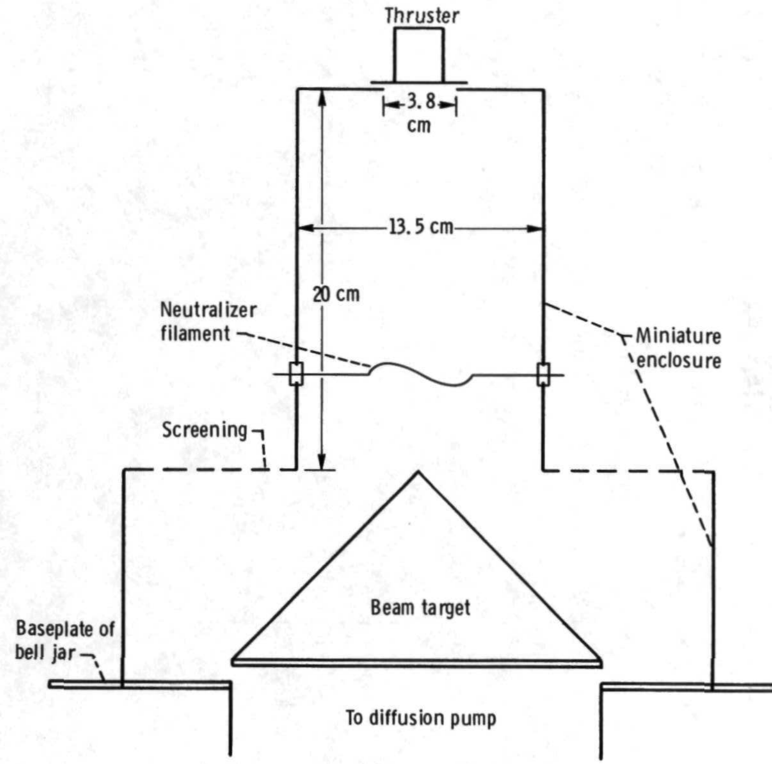


Figure 5. - Thruster setup in test bell jar.

## Thrust Level of Microthruster

Figure 6 shows the variation of required ideal beam current $J_B$ against net accelerating voltage $V_I$ for microthruster operation at three different thrust levels. The first test series, using a glass grid, was operated at a net accelerating voltage of 400 volts and a beam current of 10 milliamperes to obtain a nominal 445 micronewtons (100 $\mu$lbf) of thrust. In a later test the microthruster with a two-grid system was operated at a net accelerating voltage of 600 volts and a beam current of 9 milliamperes to give a nominal 445 micronewtons (100 $\mu$lbf) of thrust.

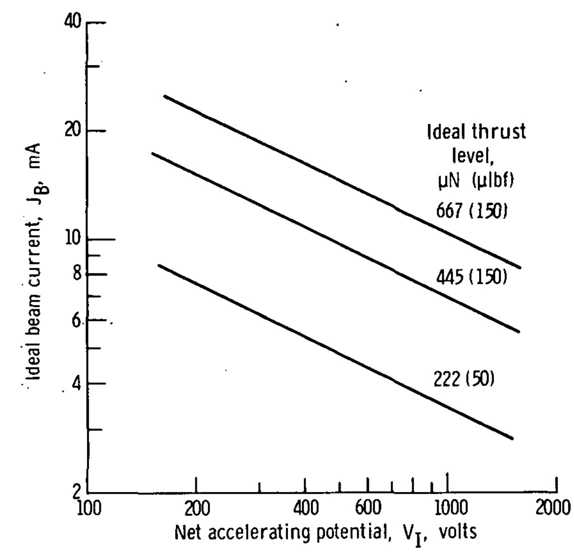


Figure 6. - Thruster beam current as function of net accelerating potential for three levels of ideal thrust (i.e., no loss due to beam divergence or double ions).

## Starting Procedure of Microthruster

The keeper - hollow-cathode discharge was lighted first, the discharge was transferred to the main anode. To light the keeper discharge with an insert-type (SERT II) hollow cathode required the tip temperature to be 1100° C as measured by the tip thermocouple, the flow of mercury to be set at a level about 25 to 50 percent above the desired beam currents, and the keeper voltage to be raised to 500 volts. With a new hollow-cathode insert the keeper discharge lighted in the order of minutes after these conditions were met. The keeper current was then set at 80 to 90 milliamperes, slightly above the operating value needed to allow the main discharge to light, and remained at this level. The keeper voltage, after lighting occurred, fell from the level of 500 volts to below 50 volts; and the discharge voltage determined by the discharge current was normally between 40 and 60 volts during operation.

## RESULTS AND DISCUSSION

### Tests of Microthruster with a Glass Grid

The first part of table I presents test data for the short microthruster with a glass grid operating with an equivalent neutral flow rate of 15.5 milliamperes. The beam current was varied from 6 to 12 milliamperes. The accelerating potentials were 400 volts for the net accelerating potential and 200 volts for the negative accelerator potential.

TABLE I. - THRUSTER OPERATING DATA

| Thruster type | Beam current, mA | Mass flow, mA | Net accelerating voltage, V | Accelerator grid | | Discharge | | Cathode keeper | |
|---|---|---|---|---|---|---|---|---|---|
| | | | | -V | mA | V | mA | V | mA |
| Short thruster, glass-coated grid | 6 | 15.5 | 400 | 200 | 0.26 | 48 | 25 | 25 | 90 |
| | 7 | | | | .28 | 49 | 28 | 52 | |
| | 8 | | | | .28 | 49 | 30 | 50 | |
| | 9 | | | | .27 | 50 | 37 | 48 | |
| | 10 | | | | .25 | 51 | 42 | 45 | |
| | 11 | | | | .24 | 52 | 50 | 40 | |
| | 12 | | | | .23 | 53 | 58 | 34 | |
| | 5 | 23 | 500 | 200 | 0.4 | 43 | 25 | 42 | 90 |
| | 7 | | | | .5 | 43 | 35 | 45 | |
| | 9 | | | | .6 | 42 | 48 | 40 | |
| | 11 | | | | .75 | | 62 | 35 | |
| | 13 | | | | .8 | | 75 | 30 | |
| | 15 | | | | .85 | | 90 | 27 | |
| | 17 | | | | .9 | | 115 | 23 | |
| | 15 | | | | .8 | | 190 | 17 | |
| Long thruster, two metal grids | 4 | 14 | 600 | 500 | 0.05 | 40 | 18 | 37 | 80 |
| | 5 | | | | .05 | 40 | 20 | 38 | |
| | 6 | | | | .06 | 41 | 22 | 43 | |
| | 7 | | | | .06 | 43 | 27 | 45 | |
| | 8 | | | | .07 | 44 | 32 | 43 | |
| | 9 | | | | .07 | 45 | 36 | 41 | |
| | 10 | | | | .08 | 47 | 41 | 39 | |
| | 11 | | | | .4 | 51 | 50 | 36 | |
| | 12 | | | | .7 | 58 | 90 | 30 | |
| | 9 | 15 | 600 | | .09 | 42 | 41 | 37 | 90 |
| (a) | 9 | 14 | 600 | | .11 | 47 | 42 | 25 | 160 |
| (b) | 9 | 14.7 | 625 | 425 | .07 | 47 | 43 | 19 | 160 |

[a]Long thruster, two metal grids, with impregnated-tip hollow cathode and smaller keeper hole.

[b]Operation of design (a) in large vacuum facility.

With a beam current of 10 milliamperes, the microthruster had a calculated thrust of 445 micronewtons (100 $\mu$lbf), which is the focal point of these data. The discharge voltages are higher than operating values of larger hollow-cathode thrusters, which operate at about 40 volts. Double ionization of the mercury propellant is greater at high discharge voltages and at 50 volts might reach values of 10 percent. This causes calculated values of thrust and propellant utilization to be somewhat higher than actual values.

Figure 7 shows discharge power per beam current as a function of propellant utilization for the microthruster operating with a glass grid. Data for the curves were taken from table I. Two curves are shown in the figure. The lower curve includes only power applied to the main discharge, while the upper curve includes the additional power of the

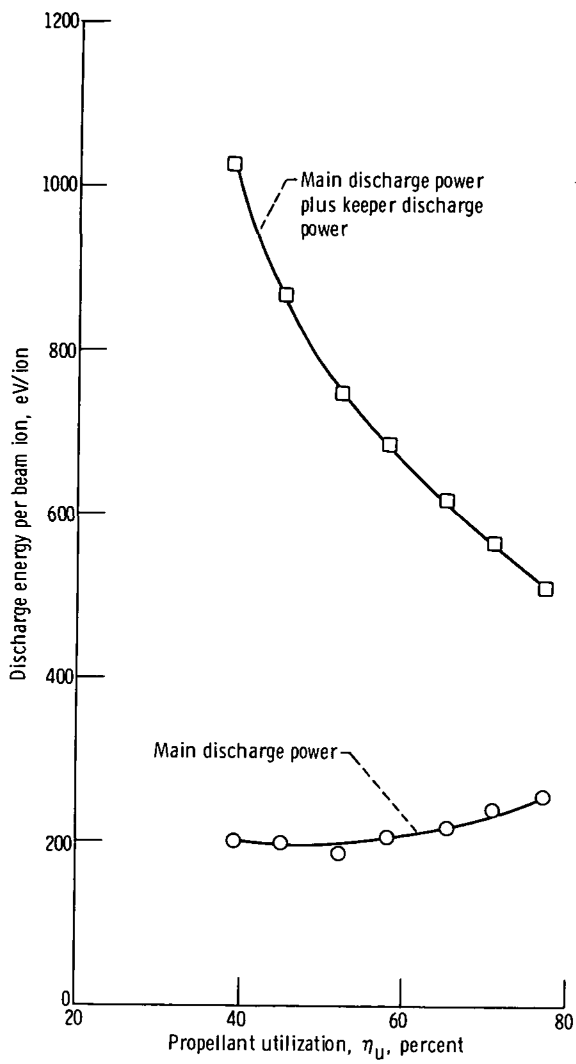


Figure 7. - Discharge energy as function of propellant utilization for short thruster with glass grid. Equivalent neutral flow, 15.5 milliamperes; net accelerating potential, 400 volts; negative accelerator potential, 200 volts.

keeper discharge. As can be seen, the keeper discharge contributed to the total discharge power of the microthruster, a power as great as and greater than the main discharge power alone. Hence, although the main discharge power scaled down in the microthruster program, the keeper power associated with the hollow cathodes used in the program did not scale down. Because the data inadvertently were ended at a beam current of 12 milliamperes, the behavior at the upper end of figure 7 was incomplete; however, later tests will show complete curves.

One of the reasons for such a large keeper power in the microthruster is the large keeper voltage. In larger-diameter thrusters, keeper voltages of the order of 10 volts are common. By using data of table I, a plot of keeper voltage against discharge power (main discharge only) is shown in figure 8. The keeper voltage dropped with increased

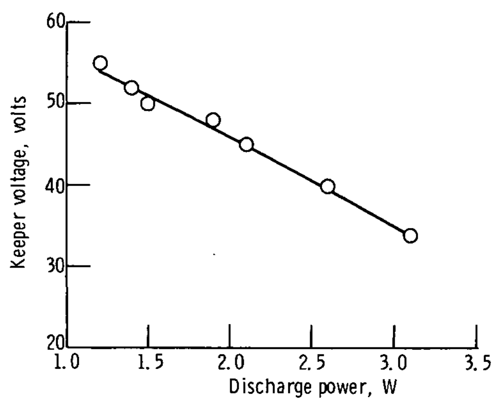


Figure 8. - Keeper voltage as function of discharge power (not including keeper power) for short thruster with glass grid. Same conditions as in figure 7.

discharge power, but relatively high values of keeper voltage existed over the entire range of discharge power.

Table II shows calculated thruster power, propellant utilization, and specific impulse for the microthrusters tested. Values in the table correspond to the 10-milliampere beam current level of table I. Assumed in this table are 7 watts power and 2 milliamperes equivalent neutral flow for a hollow-cathode neutralizer. These neutralizer conditions are the same as the type successfully operated in the 5-cm program (ref. 3). With the total thruster power of 20.1 watts, the power-thrust ratio was 45 watts per millinewton (200 W/mlbf).

One of the reasons for low thruster power of table II is that the hollow cathode was operated at zero tip heater power. Both the neutralizer and the main hollow cathode of the 5-cm thruster have operated with no tip power. High tip power, however, is needed to start the discharge; but this requirement occurs when the overall power requirement is low (thruster beam off) and is not charged against thruster efficiency. It took nominally 25 to 30 watts of tip heater power to start the thruster discharge. This power could be reduced to zero, however, in steady-state operation.

In figure 9 a curve showing the effect of varying the net accelerating voltage on the operation of the microthruster with a glass grid is presented. The beam current for this figure was 10 milliamperes at a constant flow rate of 15.5 milliamperes. The figure indicates a slight decrease in main discharge power at higher net accelerating voltages. This trend was also true when keeper power was included.

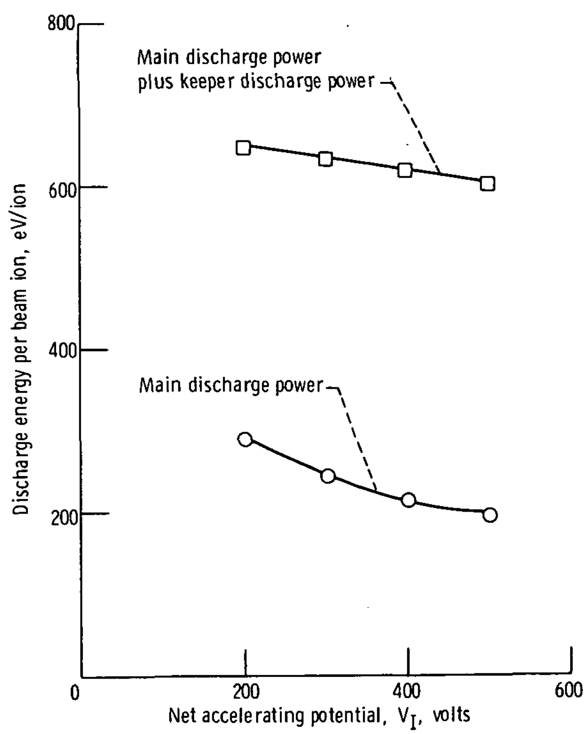


Figure 9. - Discharge energy as function of net accelerating potential for short thruster with glass grid. Equivalent neutral flow, 15.5 milliamperes; beam current, 10 milliamperes; negative accelerator potential, 200 volts.

Data for the short microthruster operating with an equivalent neutral flow of 23 milliamperes are presented in the middle of table I. The beam current was varied from 5 to 17 milliamperes, the maximum obtainable, for these data. The net accelerating potential was 500 volts, and the negative accelerator potential was 200 volts. The main discharge voltages are lower in these data than in the previous data. The keeper voltages for the high-beam-current values are also lower than for similar operation for the previous data.

An interesting feature of the data is that increased discharge power (the product of discharge voltage and current) produced higher beam currents, to a maximum of 17 milliamperes. Further increase of discharge power, however, resulted in an actual recorded dip of the beam current. Similar operating features have been encountered in other tests with hollow-cathode bombardment thrusters and, when they occur, must be considered in thruster control logic.

Figure 10 is a plot of discharge energy per beam ion as a function of propellant utilization. Data for the plot were taken from table I. Only the main discharge power

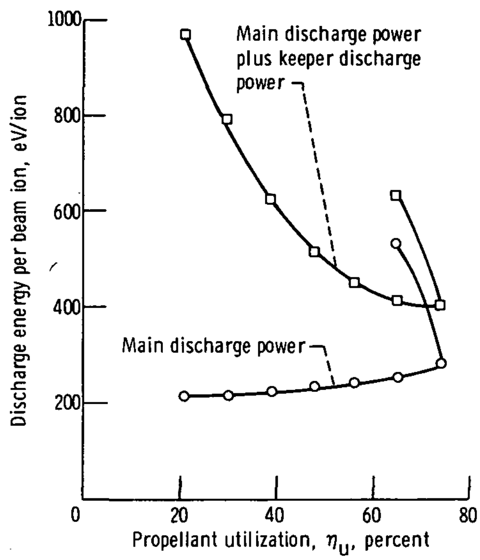


Figure 10. - Discharge energy as function of propellant utilization for short thruster with glass grid. Equivalent neutral flow, 23 milliamperes.

is included in the lower curve. From the curves it can be seen that the microthruster has a maximum propellant utilization of 74 percent. Because the data are made up of low discharge voltages, double ionization is not a factor. This maximum value of 74 percent is lower than is found in larger thrusters of similar design and is in qualitative agreement with the maximum utilization theory of reference 11.

By taking the optimum operating point from table I corresponding to a 17-milliampere beam current, the values of table II were calculated. Total thruster power was 25.3 watts at a calculated thrust of 800 micronewtons (180 $\mu$lbf), resulting in a power-thrust ratio of 31.5 watts per millinewton (140 W/mlbf).

## Tests of Microthruster with Two-Grid System

Performance data and power requirements. - Electron bombardment thruster tests using a SERT II design and a glass grid have resulted in high-performance, low-specific-impulse operation, as can be seen, for example, in reference 12. However, as indicated in reference 9, high-performance operating with a glass grid has been found to be dependent on facility backsputtering onto the glass holes. In addition, discharge-chamber sputtered deposits condensing on the glass grids may seriously limit glass-grid lifetime. Therefore, low-specific-impulse, high-performance, two-grid systems have been reemphasized. Thus, the microthruster underwent further tests with a low-specific-impulse, high-performance, two-grid system. A high-open-area, close-spaced, thin-screen-grid, two-grid system previously described was used.

Although the two-grid system used had a mica spacer for testing, the incorporation of a spaceworthy mount design would not be a major problem. In addition, the use of two, thin, flat grids does not present a thermal buckling problem because of the small aspect ratio of this small-diameter thruster.

In this test series, a longer thruster was chosen for testing based on the hypothesis that a larger-volume discharge plasma would have a lower impedance and, hence, a lower discharge voltage.

The lower part of table I presents test data for the long thruster with a two-grid system operating with an equivalent neutral flow rate of 14 milliamperes. For one test at 14-milliampere flow rate, a hollow cathode with a new insert was used and, for these performance measurements, was operated at a tip heater power of about 10 watts. Later, however, it was found that operation with zero tip heat was possible; and, therefore, for power measurements, the thruster was run with no tip heater power. The beam current in the test was varied between 4 and 12 milliamperes. The accelerating potentials were necessarily higher for this two-grid system than for the similar run with a glass grid presented in the upper part of table I. For the accelerating potential used here, a beam current of 9 milliamperes corresponds to a calculated thrust level of 445 micronewtons (100 $\mu$lbf). The discharge voltages, as expected, are lower in this test than in the test represented by table I. This is true for comparisons made between similar operating values of propellant utilization.

Figure 11 represents chamber performance data for operation of the microthruster with a two-grid system plotted from the data of table I. The curves of figure 11 depict main and total discharge energy per beam ion as a function of propellant utilization. As with previous data for the thruster with a glass grid, the keeper discharge represents a significant portion of the total discharge power, as can be seen in the upper curve of figure 11. This curve of total chamber power decreases with increasing beam until a minimum is reached. The minimum corresponds to the knee of the lower curve.

From the data of table I, two plots, shown in figures 12 and 13, were made. Figure 12 shows a curve of discharge voltage as a function of beam current. Simply stated, higher discharge voltages are required for increases in beam current at a constant neutral flow rate. In figure 13, discharge current is shown as a function of discharge volt-

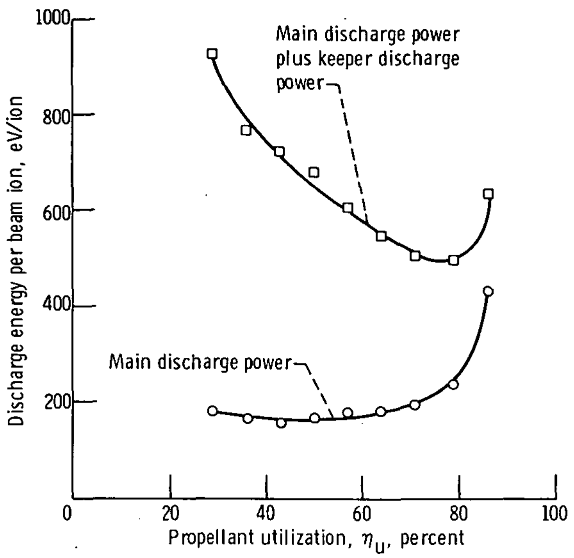


Figure 11. - Discharge energy as function of propellant utilization for long thruster with two-grid system. Equivalent neutral flow, 14 milliamperes; net accelerating potential, 600 volts; negative accelerator potential, 500 volts. Data from table I.

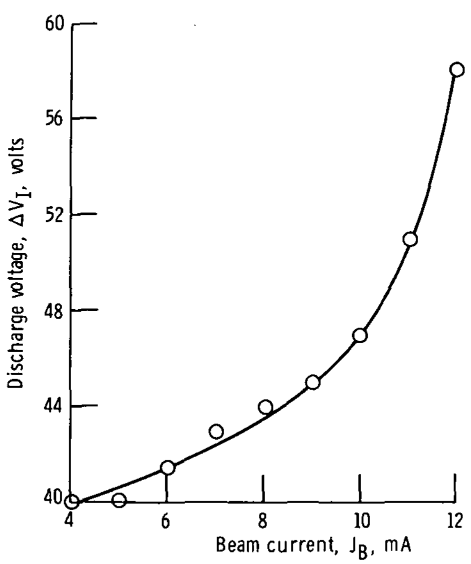


Figure 12. - Discharge voltage as function of beam current for long thruster with two-grid system. Same conditions as in figure 11.

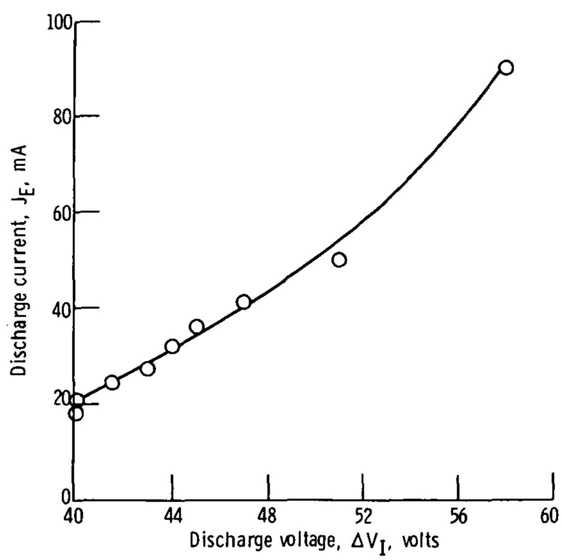


Figure 13. - Discharge current as function of discharge voltage for long thruster with two-grid system. Same conditions as in figure 11.

age, for the microthruster with an extracted beam current. The plot shows a monotonic increase of discharge current with increasing discharge voltage.

Table I presents data for the long thruster with a two-grid system operating at a thrust level of 445 micronewtons (100 $\mu$lbf) and a flow rate of 15 milliamperes. The thruster hollow cathode was operated at zero tip heater power as stated before, and thruster parameters and power requirements were recorded. Comparing data of this run with the similar beam current data in table I shows some small variations. The impingement current is slightly higher in this test but is within a normal value of 1 percent of the beam current. The discharge voltage was somewhat lower at 42 volts, and the keeper power varied only slightly between tests. The total thruster power including an assumed hollow-cathode neutralizer for the test run was 20.4 watts with a propellant utilization of 53 percent, and the power-thrust ratio was 46 watts per millinewton (204 W/mlbf).

Tests of impregnated-tip hollow cathodes. - After about 20 test runs (including startups) with the microthruster using the initial hollow cathode, it became impossible to operate the thruster at zero tip heater power. This problem was eliminated by installing a new hollow-cathode insert. Zero-tip-heat operation has been shown in the 5-cm program and in the microthruster program, but zero tip heat was not maintained throughout this test. Although the SERT II program showed consistent hollow-cathode behavior when strict test procedures were used, the requirement of zero tip heat was not included in that program.

Three difficulties of maintaining zero-tip-heat performance are (1) the hydroscopic barium oxide (BaO) formed on activation of a hollow cathode can physically flake off on opening to atmosphere; (2) the activated surface might be chemically poisoned either during running or on opening to atmosphere; and (3) sputtering or evaporation due to ion bombardment or startup may destroy the activated surface during hollow-cathode operation.

Therefore, a differently designed hollow-cathode tip was tried. The tip of this hollow cathode was made of BaO-impregnated tungsten, and no insert was used. Impregnated, porous tungsten cathodes can be exposed to air and be reused with possibly less damage to the activated surface than present designs. The impregnated tip, presumably, might be able to be gradually surface-worn by sputtering and still maintain activation.

Table II compares the operation of the microthruster with the impregnated hollow-cathode tip with the operation of a similar microthruster with a SERT II-type hollow cathode. In addition, in this test and in further tests, a smaller keeper hole (0.32-cm diam instead of a 0.64-cm diam) was used and resulted in a lower keeper voltage. Accelerating potentials, beam currents, discharge powers, and impingement current are quite similar in both test runs. The microthruster with the impregnated tip would not, however, operate without tip heater power or below about 700° C tip temperature. In fact, after a number of test runs the required heater power seemed to level off at a

TABLE II. - CALCULATED THRUSTER PERFORMANCE

| | Short thruster with glass-coated grid | | Long thruster with two metal grids |
|---|---|---|---|
| Thrust[a], $\mu$N ($\mu$lbf) | 410 (92) | 777 (175) | 450 (101) |
| Thruster power, W: | | | |
| Beam | 4.0 | 8.5 | 5.4 |
| Discharge | 2.1 | 4.8 | 1.7 |
| Keeper | 4.0 | 2.0 | 3.3 |
| Vaporizer | 3.0 | 3.0 | 3.0 |
| Cathode | 0.0 | 0.0 | 0.0 |
| Neutralizer (est.) | (7.0) | (7.0) | (7.0) |
| Total power | 20.1 | 25.3 | 20.4 |
| Propellant utilization (including neutralizer) | 0.60 | 0.68 | 0.53 |
| Specific impulse, sec | 1200 | 1520 | 1300 |
| Power-thrust ratio, W/mN (W/mlbf) | 49 (218) | 33 (145) | 45 (202) |

[a]Ideal thrust, no loss assumed for beam divergence or double ions.

heater power somewhat higher than recorded in table I. The impregnated-tip cathode, however, consistently lighted after a number (5 to 10) of runs and after a number of openings to atmosphere. This is not typical for hollow cathodes with coated tips (activator applied to tip rather than insert). The thruster operation with this hollow cathode maintained the same type of performance as the microthruster with a SERT-type hollow cathode. A simple improvement to the impregnated hollow cathode can be suggested. That is the use of an impregnated insert instead of an impregnated tip. This approach has resulted in zero-tip-heat operation in a simulated ion thruster (private communication from H. Hudson of Lewis Research Center).

Discharge sensitivity to neutral flow rate. - It was observed in the running of the microthruster and has been observed in other hollow-cathode thrusters that the discharge voltage was sensitive to neutral flow rate (ref. 12). A test run to document this behavior was made and results are shown in figure 14. The beam current was held at 9 milliamperes. Flow rates varied from 13.5 to 18 milliamperes. As a result of the variation of flow rate, a variation of discharge voltage occurred with increased flow rate, causing decreased discharge voltage. Thus, it can be stated that geometric designs must be matched to flow rate in order to maintain a set discharge voltage.

Two-grid system test. - A test of grid perveance for the microthruster with a

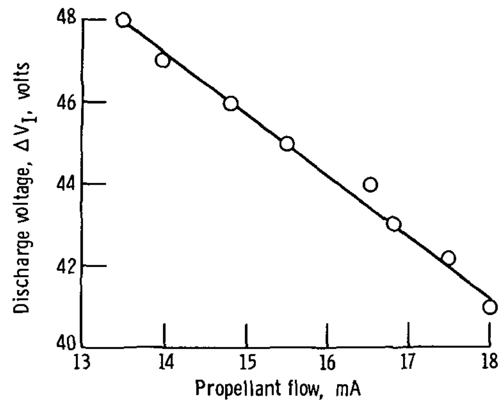


Figure 14. - Discharge voltage as function of propellant flow for long thruster with two-grid system and an impregnated-tip cathode. Beam current, 9 milliamperes; net accelerating voltage, 600 volts; negative accelerator potential, 500 volts.

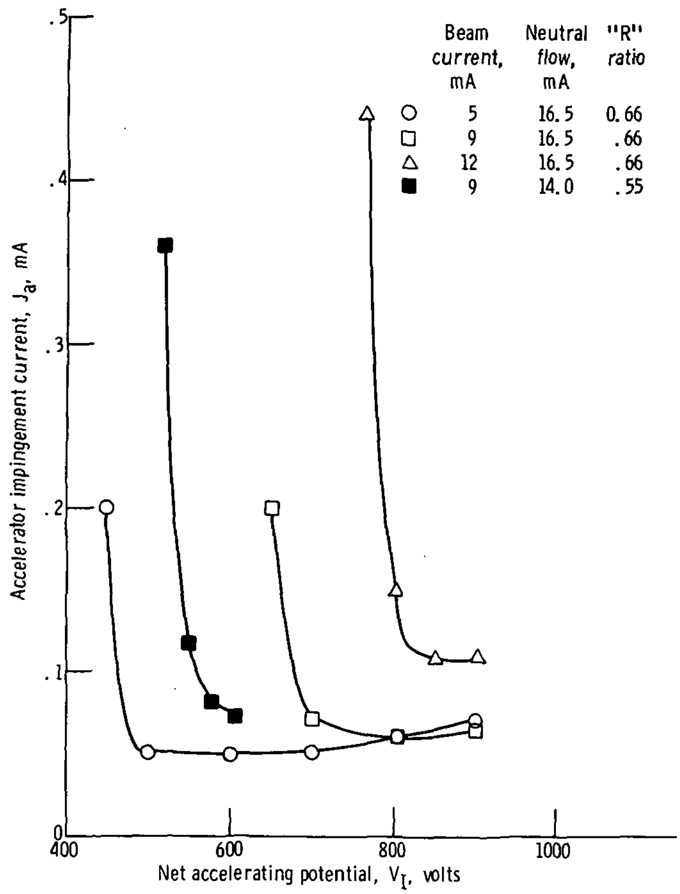


Figure 15. - Accelerator impingement current as function of net accelerating voltage for long thruster with two-grid system. Grid separation, 0.05 centimeter; "R" = $V_I/(V_I + V_A)$, where $V_A$ is negative accelerator potential.

two-grid system was made. Figure 15 is a plot of accelerator grid impingement curves for beam currents of 5, 9, and 12 milliamperes. Data were taken as in reference 13. The curves show net accelerating voltages below which the microthruster could not operate with low impingement. The maximum net accelerating voltage was the power supply limit. The "R" ratio for each curve was constant. ("R" is defined as the ratio of net-to-total accelerating voltages.) Figure 16 is a log-log plot of beam current against total accelerating voltage at the knee of the curves in figure 15. A straight line through the three points of figure 16 has a slope of 1.7, which compares to 1.5 power dependence of Child's law. The grid data, if compared on the basis of beam current density, agree well with the low-specific-impulse data of reference 14.

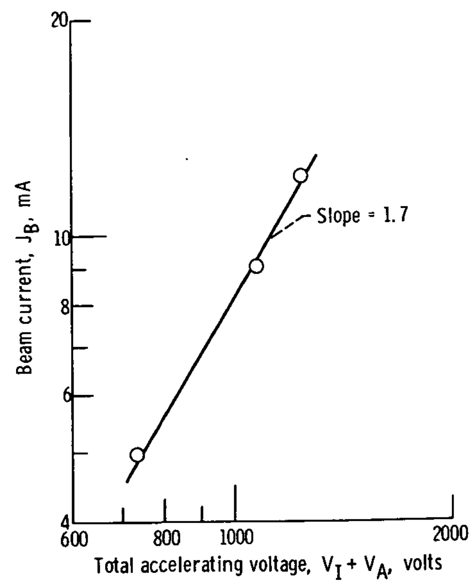

Figure 16. - Beam current of figure 15 as function of total accelerating voltages at the knee.

Impingement current is also shown for operation at 14-milliampere flow rate and an "R" ratio corresponding to the 14-milliampere flow rate data of table I. The 9-milliampere beam current of figure 15 had a "knee voltage" only 50 volts lower than the accelerating voltages of table I. Therefore, at beam currents larger than 9 milliamperes, the impingement current increases, as indicated in table I.

Large facility test. - As a last test the impregnated-tip microthruster was operated in a vacuum tank of the size used to test thrusters of 5 to 30 centimeters in diameter. No significant difference in operation was found, as can be seen in a comparison of the last two rows of table I. Furthermore, a test run of 6 hours duration was made with the microthruster in the large vacuum facility. Besides a "discharge out" at the 4-hour mark and a restart at that point, no anomalies were noticed. Also, long-duration flow measurements indicated no variation of data from previous tests.

## CONCLUSIONS

A 2.5-centimeter-diameter Kaufman microthruster was fabricated and tested. Discharge power per beam ion for the microthruster had similar low values as for larger, advanced-design thrusters when power to the main anode was the only consideration. However, the inclusion of keeper power as part of the discharge power resulted in large total discharge powers as compared to the larger thrusters. When double ionization was kept low, propellant utilization showed a maximum value lower than is found in large advanced-design thrusters, in agreement with theory.

The microthruster was able to operate stably with no hollow-cathode tip heat although relatively large tip powers were necessary for starting. As a result, the microthruster at a 445-micronewton (100-$\mu$lbf) thrust level was able to operate with the use of less than 30 watts of electrical power. The steady-state operating power included an assumed 7 watts for neutralizer operation. Although a glass grid was initially used for the microthruster tests, a low-specific-impulse, two-grid system was successfully incorporated into the design. The program showed that an electron bombardment microthruster for an auxiliary mission with a thrust level of approximately 445 micronewtons (100 $\mu$lbf) could be successfully operated.

Lewis Research Center,
National Aeronautics and Space Administration,
Cleveland, Ohio, October 16, 1972,
502-24.

## REFERENCES

1. Isley, William C.; and Mickelsen, William R.: Electric Microthrusters Make It. Astronautics & Aeronautics, vol. 6, no. 6, June 1968, pp. 54-61.

2. Nakanishi, S.; Lathem, W. C.; Banks, B. A.; and Weigand, A. J.: Status of a Five-Centimeter-Diameter Ion Thruster Technology Program. Paper 71-690, AIAA, June 1971.

3. Hyman, Julius, Jr.: Design and Development of a Small Structurally Integrated Ion Thruster System. Hughes Research Labs. (NASA CR-120821), Oct. 1971.

4. Boucher, Roland A.: Electrical Propulsion for Control of Stationary Satellites. J. Spacecraft Rockets, vol. 1, no. 2, Mar.-Apr. 1964, pp. 164-169.

5. Bechtel, Robert T.: Discharge Chamber Optimization of the SERT II Thruster. J. Spacecraft Rockets, vol. 5, no. 7, July 1968, pp. 795-800.

6. Kerslake, W. R.; Goldman, R. G.; and Nieberding, W. C.: SERT II: Mission, Thruster Performance, and In-Flight Thrust Measurements. J. Spacecraft Rockets, vol. 8, no. 3, Mar. 1971, pp. 213-224.

7. Bechtel, R. T.: Performance of a Neutralizer for Electron Bombardment Thruster. Paper 72-207, AIAA, Jan. 1972.

8. Banks, Bruce: Composite Ion Accelerator Grids. NASA TM X-52425, 1968.

9. Bechtel, R. T.; Banks, B. A.; and Reynolds, T. W.: Effect of Facility Backsputtered Material on Performance of Glass-Coated Accelerator Grids for Kaufman Thrusters. Paper 71-156, AIAA, Jan. 1971.

10. Bechtel, R. T.; Csiky, G. A.; and Byers, D. C.: Performance of a 15-Centimeter Diameter, Hollow-Cathode Kaufman Thrustor. Paper 68-88, AIAA, Jan. 1968.

11. Kaufman, H. R.; and Cohen, A. J.: Maximum Propellant Utilization in an Electron-Bombardment Thruster. NASA TM X-67921, 1971.

12. Bechtel, Robert T.: Performance and Control of a 30-Centimeter Diameter, Low-Impulse, Kaufman Thruster. J. Spacecraft Rockets, vol. 7, no. 1, Jan. 1970, pp. 21-25.

13. Kerslake, William R.: Accelerator Grid Tests on an Electron-Bombardment Ion Rocket. NASA TN D-1168, 1962.

14. Rawlin, V. K.; Banks, B. A.; and Byers, D. C.: Design, Fabrication, and Operation of Dished Accelerator Grids on a 30-Centimeter Ion Thruster. Paper 72-486, AIAA, Apr. 1972.

NATIONAL AERONAUTICS AND SPACE ADMINISTRATION
WASHINGTON, D.C. 20546

OFFICIAL BUSINESS
PENALTY FOR PRIVATE USE $300

SPECIAL FOURTH-CLASS RATE
BOOK

POSTAGE AND FEES PAID
NATIONAL AERONAUTICS AND
SPACE ADMINISTRATION
451

U.S. MAIL

POSTMASTER: If Undeliverable (Section 158 Postal Manual) Do Not Return

---

*"The aeronautical and space activities of the United States shall be conducted so as to contribute . . . to the expansion of human knowledge of phenomena in the atmosphere and space. The Administration shall provide for the widest practicable and appropriate dissemination of information concerning its activities and the results thereof."*

—NATIONAL AERONAUTICS AND SPACE ACT OF 1958

# NASA SCIENTIFIC AND TECHNICAL PUBLICATIONS

TECHNICAL REPORTS: Scientific and technical information considered important, complete, and a lasting contribution to existing knowledge.

TECHNICAL NOTES: Information less broad in scope but nevertheless of importance as a contribution to existing knowledge.

TECHNICAL MEMORANDUMS: Information receiving limited distribution because of preliminary data, security classification, or other reasons. Also includes conference proceedings with either limited or unlimited distribution.

CONTRACTOR REPORTS: Scientific and technical information generated under a NASA contract or grant and considered an important contribution to existing knowledge.

TECHNICAL TRANSLATIONS: Information published in a foreign language considered to merit NASA distribution in English.

SPECIAL PUBLICATIONS: Information derived from or of value to NASA activities. Publications include final reports of major projects, monographs, data compilations, handbooks, sourcebooks, and special bibliographies.

TECHNOLOGY UTILIZATION PUBLICATIONS: Information on technology used by NASA that may be of particular interest in commercial and other non-aerospace applications. Publications include Tech Briefs, Technology Utilization Reports and Technology Surveys.

*Details on the availability of these publications may be obtained from:*

SCIENTIFIC AND TECHNICAL INFORMATION OFFICE

NATIONAL AERONAUTICS AND SPACE ADMINISTRATION

Washington, D.C. 20546